1981ApJ...244..869D

THE ASTROPHYSICAL JOURNAL, 244: 869–883, 1981 March 15
© 1981. The American Astronomical Society. All rights reserved. Printed in U.S.A.

OUTFLOW OF MATTER IN THE KL NEBULA: THE ROLE OF IRc2

D. DOWNES,[1,5] R. GENZEL,[2,5] E. E. BECKLIN,[3,4] and C. G. WYNN-WILLIAMS[3,5]
Received 1980 June 24; accepted 1980 October 1

ABSTRACT

New observations have been made of the Orion-KL Nebula with the Infrared Telescope Facility on Mauna Kea at 8.7 μm and 20 μm with 2″ resolution. The maps show many new infrared peaks, with good correlation with H_2O masers, as well as 20 μm emission reaching to the outermost peaks of the 2 μm molecular hydrogen emission. New spectrophotometric measurements of the stronger peaks in the range 4.8–20 μm show that the compact source IRc2 has a very deep silicate feature with $\tau_{9.7\ \mu m} \gtrsim 5$, and hence that its luminosity has been hitherto seriously underestimated. The other infrared peaks have silicate absorption comparable with that of the BN object ($\tau_{9.7\ \mu m} \approx 0.5$–1). IRc2 and BN are "hot" sources with color temperatures $\gtrsim$350 K over 8–20 μm, while the other features of the KL Nebula have $T_c \sim 120$–150 K. The infrared observations suggest that IRc2 is a star of 10^4–10^5 $L_\odot$ and is the primary source of energy for all of the outflow phenomena seen in molecular-line spectra. The rate of mass loss in the outflow from IRc2 is $\sim 10^{-4}$–10^{-3} $M_\odot$ yr^{-1}, continuous over the past 10^3 to 10^4 years; the mass contained in the flow is $\sim$1–10 $M_\odot$. IRc2 may be a young, massive star in the last stages of its formation rather than an evolved star. The high rate of mass loss prevents the formation of a compact H II region and the clearing out of a large, ionized cavity in KL. The mass loss from IRc2 and BN could account for their dust envelopes, their strong infrared emission, and their high visual extinction. Heating by the radiation and outflow from IRc2 may be responsible for the infrared appearance of the KL nebula.

Subject headings: infrared: sources — masers — nebulae: individual — nebulae: Orion Nebula — stars: mass loss

I. OBSERVATIONS

a) Introduction

This paper presents new maps at high resolution and high sensitivity of the Kleinmann-Low Nebula in Orion at 8.7 μm and 20 μm, as well as broad-band photometry of the stronger sources. This work was motivated by the recent VLBI measurements of proper motions of the Orion H_2O masers, by the identification of the Orion SiO maser with the infrared source IRc2, and by proposals that the molecular "plateau source" may be explained by mass loss of some sort from a star or stars in the KL Nebula (e.g., Zuckerman, Kuiper, and Rodriguez-Kuiper 1976; Genzel and Downes 1977; Hall *et al.* 1978; Scoville 1980). Section II of this paper describes our infrared results. Section III presents a new interpretation of the KL Nebula based on infrared and molecular-line data. Section IV explores the consequences of this picture for the interpretation of H_2O masers. Section V discusses the wider implications of the Orion results for regions of star formation throughout the Galaxy.

b) Observing Method

The observations were made at Mauna Kea, Hawaii, in 1980 February with a gallium-doped germanium bolometer mounted on the 3 m Infrared Telescope Facility (IRTF). We mapped the central region of the KL Nebula (Fig. 1, solid contours) at 20 μm with a beam of 2″.3 × 1″.9 (R.A. × decl.) and adjacent regions (Fig. 1, dashed contours) with a beam of 4″. We also mapped the central region at 8.7 μm with a beam of 2″.2 × 1″.9 (Fig. 2). The bandwidths at 20 and 8.7 μm were 9 and 1.2 μm, respectively. The grid spacing was one-half beamwidth in all cases, and the peak-to-peak sensitivity was 4 Jy at 20 μm and 1 Jy at 8.7 μm. The tracking stability of the telescope was better than 1″ over 10–20 minutes, which permitted us to map with positional accuracy ~0″.5 relative to the Becklin-Neugebauer object.

We determined the position of the BN object at 2.2, 8.7, and 20 μm by offsetting from θ^1 Ori C, for which we adopted the position of SAO 132314 in the SAO Catalogue (1966). The resulting position of BN (Table

[1]Institut de Radio Astronomie Millimetrique, Grenoble, France.
[2]Harvard-Smithsonian Center for Astrophysics, Cambridge, Massachusetts.
[3]Institute for Astronomy, University of Hawaii.
[4]Staff Astronomer, Infrared Telescope Facility.
[5]Visiting Astronomer, Infrared Telescope Facility, operated by the University of Hawaii for the National Aeronautics and Space Administration.

© American Astronomical Society • Provided by the NASA Astrophysics Data System

1981ApJ...244..869D

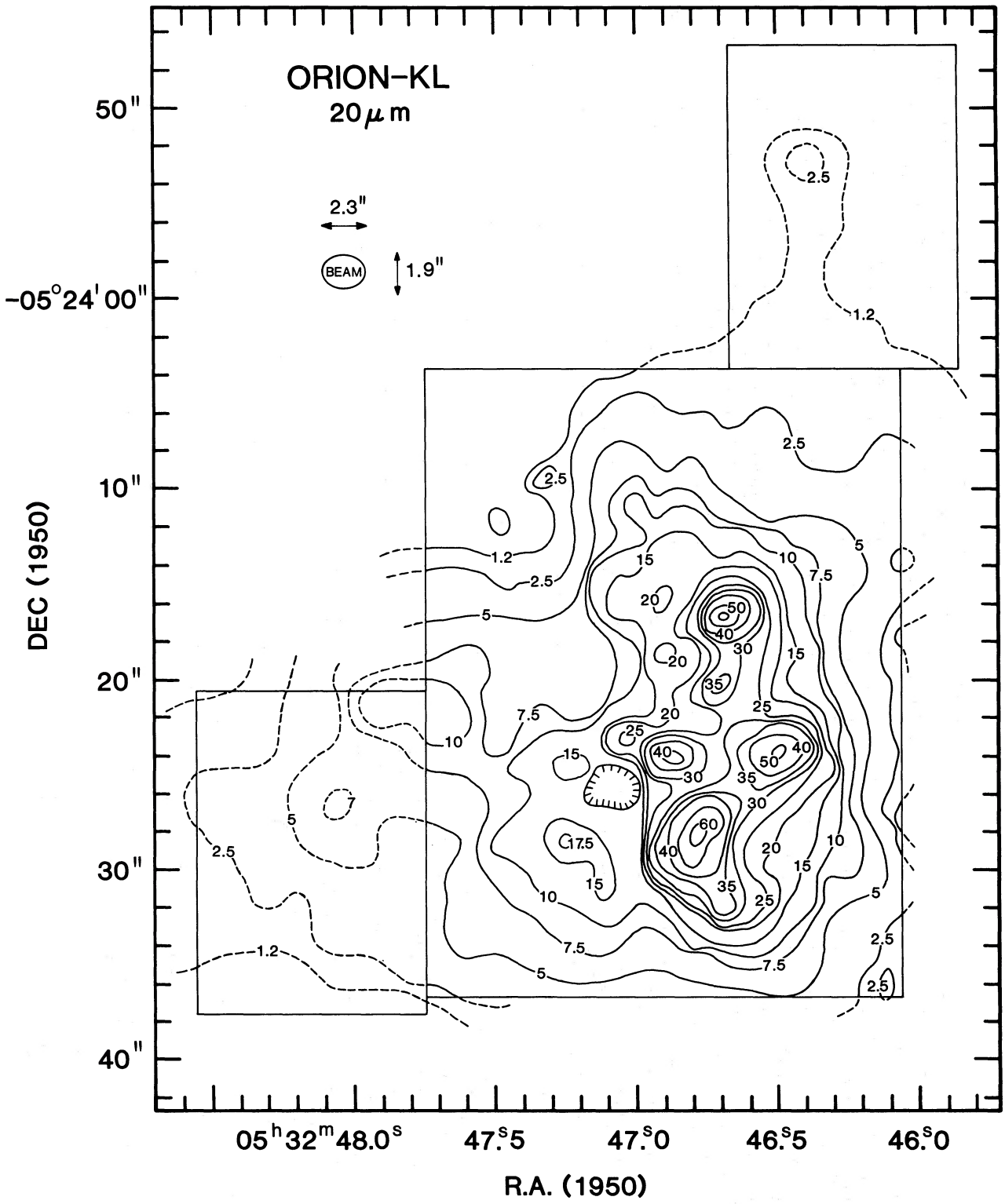

FIG. 1.—Map of the KL Nebula at a wavelength of 20 μm. The contour unit is 1.30 10^{-15} W m^{-2} Hz^{-1} sr^{-1}, or 10.5 Jy from an equivalent point source. The *rectangles* mark the areas mapped. The central region (*solid contours*) was observed with 2″ resolution, the outer regions (*dashed contours*) with 4″ resolution.

© American Astronomical Society • Provided by the NASA Astrophysics Data System

1981ApJ...244..869D

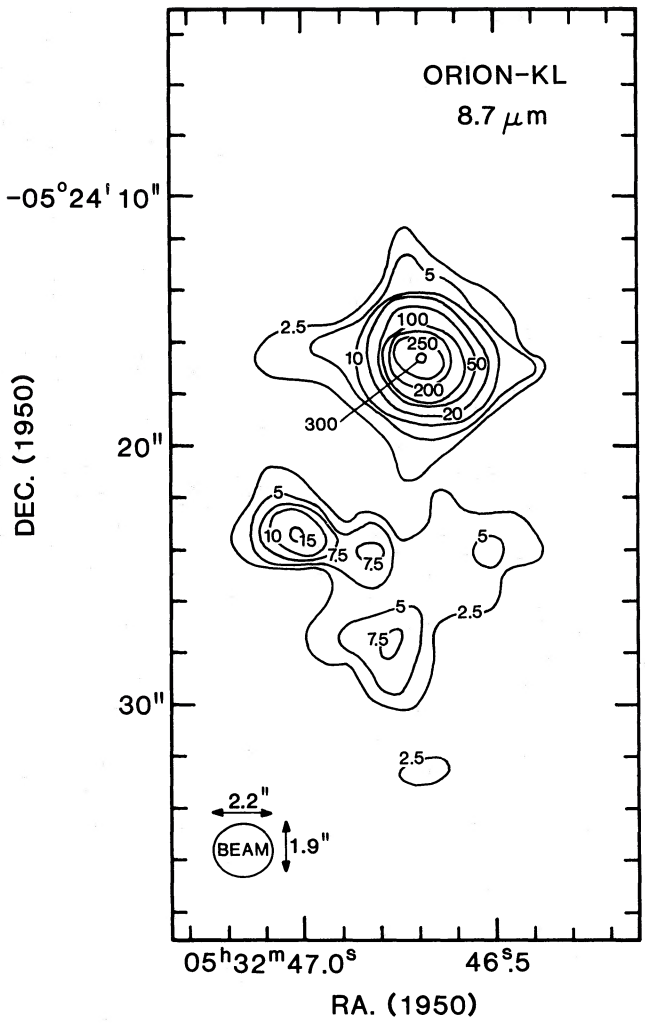

FIG. 2.—Map of the central region of the KL Nebula at a wavelength of 8.7 μm. The contour unit is 9.13 10^{-17} W m^{-2} Hz^{-1} sr^{-1}, or 0.7 Jy from an equivalent point source. The two lowest contours of the BN source may be influenced by diffraction from the supports of the secondary mirror.

TABLE 1

POSITIONS AND FLUXES OF THE STRONGER INFRARED PEAKS

SOURCE NAME	1950 POSITION R. A. 05^h32^m	1950 POSITION Decl. $-05°24'$	UNCORRECTED HALF-POWER WIDTH R. A. (arcsec)	UNCORRECTED HALF-POWER WIDTH Decl. (arcsec)	FLUX DENSITY IN A 2″ BEAM (INCLUDING BACKGROUND) 20 μm (Jy)	FLUX DENSITY IN A 2″ BEAM (INCLUDING BACKGROUND) 8.7 μm (Jy)	REMARKS
IRc1 = BN ..	46.69	16″.6	2	2	630	220	Point source
IRc2	47.03	23.2	2	2	260	12	Point source; SiO maser
IRc3	46.51	23.9	4	3	530	4	...
IRc4	46.78	28.0	3	4	630	6	...
IRc5	46.7	33.0	4	3	370	2	...
IRc6	46.7	20.2	...	...	370	2	New source 4″ south of BN
IRc7	46.85	24.0	3	2	420	6	New source 3″ west of IRc2
IRc8	47.26	28.6	...	...	180	...	Peak in extended ridge; spectrum in Fig. 4
IRc9	46.4	23′52″.7	2	2	25	...	Point source (IRS2; Wynn-Williams and Becklin 1974)

© American Astronomical Society • Provided by the NASA Astrophysics Data System

1981ApJ...244..869D

1) was the same at all three wavelengths and, to within the accuracy of $\pm 0''.5$, agrees with the position originally measured by Becklin and Neugebauer (1968).

We also made spectrophotometric measurements of some of the stronger sources, with a 4″ beam, at effective wavelengths of 20 μm ($\Delta\lambda = 9$ μm), 18.3 μm ($\Delta\lambda = 6$ μm), 12.5, 11.6, 9.7, and 8.7 μm (all with $\Delta\lambda = 1.2$ μm), 7.9 μm ($\Delta\lambda = 0.7$ μm), and 4.8 μm ($\Delta\lambda = 0.4$ μm). The photometry was calibrated relative to μ UMa and α Tau. In both the mapping and photometry, the throw of the chopping secondary was 30″ E-W.

II. RESULTS

a) *Comparison with Other Infrared Maps*

The previous infrared maps of the KL Nebula with the highest angular resolution were those published by Rieke, Low, and Kleinmann (1973) and Wynn-Williams and Becklin (1974). A new map has also been made with the Wyoming telescope by Grasdalen *et al.* (1980). The new IRTF maps presented here have higher resolution and sensitivity than the earlier maps. In particular, there is good resolution for the first time of the compact sources at 20 μm, which were previously blended together in the older 20 μm maps with 5″ beams. The source IRc2, for example, was visible only as a bulge in the extended contours on the 21 μm map by Rieke *et al.*

Several of the stronger infrared peaks are listed in Table 1. We follow the source nomenclature of Rieke *et al.* for IRcl through IRc5 and add new designations IRc6 through IRc9. Positional errors in right acension and declination are ($\pm 0^s.03, \pm 0''.5$) for IRcl (the BN object), and ($\pm 0^s.05, \pm 0''.7$) for the other sources. The half-power widths are uncorrected for broadening by the 2″ beam, and the flux densities are the values measured with the 2″ beam and 30″ E-W chopper throw, with no correction for any contribution from the extended background.

While there is good agreement with the maps of Rieke *et al.* and Wynn-Williams and Becklin for the main peaks, there are a number of new results from the IRTF maps:

1. The source IRc2 is resolved by our 2″ beam into two peaks, the easternmost of which is the dominant source at 8.7 μm (Fig. 2). In what follows, we refer to this eastern, "hot" component as IRc2 and the western, "cool" component as IRc7.

2. At 20 μm there is a new, compact peak, IRc6, located ~4″ south of the BN object. There may have been an earlier hint of the existence of this component in the asymmetry of the 20 μm contours of BN on the maps by Rieke *et al.* and Wynn-Williams and Becklin.

3. There is a discrepancy in the position of the source labeled IRc5 by Rieke *et al.* On their 20 μm map, the source appears as a ridge to the south*east* of IRc4, while on our map (Fig. 1) it lies to the south*west*, giving a much improved agreement with the positions of the H_2O maser in that region.

4. The mapping and photometry show that a number of the 20 μm peaks are extended. In particular, IRc3 and IRc4 are spatially resolved, in contrast to BN and IRc2 which are unresolved on our maps and which, therefore, must have diameters $< 1''$ at 20 μm.

5. In addition to the compact sources, there is an extended background at 20 μm with two components: a central region of size 10″ × 20″ (R.A. × decl.) and a more extended, weaker nebula, roughly triangular in shape, over 40″ × 40″. At 20 μm, there are numerous compact knots embedded in the extended background. The 20 μm map shows nicely the relative strengths of the BN object and the extended background radiation in the vicinity of BN. On the peak of BN, the intensity is 630 Jy in a 2″ beam, of which ~430 Jy comes from the unresolved source, and ~200 Jy comes from the extended background.

b) *Spectra*

The spectra of the sources over 4.8–20 μm are shown in Figures 3 and 4. Because our 30″ chopper

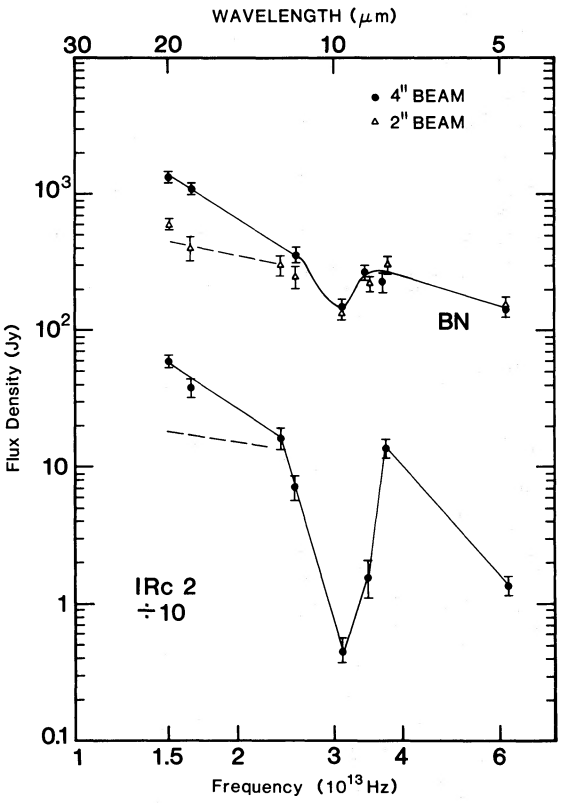

FIG. 3.—Near-infrared spectra of the BN object and IRc2. *Solid lines* show the uncorrected flux densities in a 2″ or 4″ beam, *dashed lines* show how the spectra would look if the intensity of the extended "background" were to be subtracted from the measured fluxes.

© American Astronomical Society • Provided by the NASA Astrophysics Data System

1981ApJ...244..869D

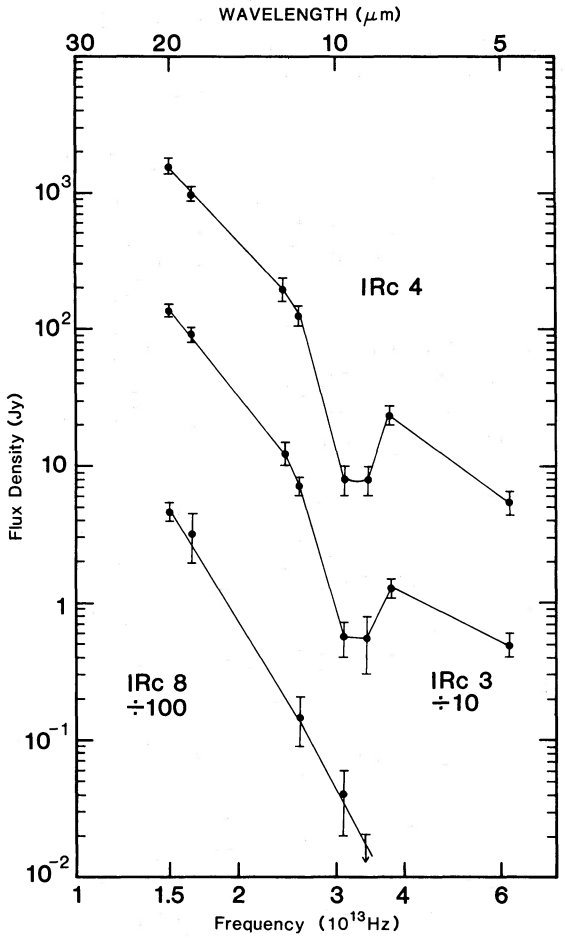

FIG. 4.—Spectra of IRc3, IRc4, and IRc8. The flux densities were measured with a 4″ beam, and no correction was made for any "background."

throw does not eliminate the extended background of the KL Nebula, the flux densities measured for some sources at 20 μm are higher than the previous values in the literature. We estimated the intensity of the background adjacent to the individual sources by constructing right acension and declination profiles from our 20 μm map. The solid lines in Figures 3 and 4 are the uncorrected spectra, including the background, while the dashed lines in Figure 3 represent the measured spectra of BN and IRc2, minus the extended background.

A further comparison may be made of the peak fluxes on the 8.7 μm map made with a 2″ beam, and the fluxes obtained in the spectrophotometry with a 4″ beam. For IRc2, for example, the fluxes in 2″ and 4″ beams are equal, which shows that, at this wavelength, the photometric data refer to the unresolved source and do not include any significant contribution from the extended background or from the nearby source IRc7.

Figures 3 and 4 show that BN and IRc2 have higher color temperatures (300–500 K between 8 and 20 μm) than the other sources in the region. IRc3, IRc4, and the extended ridge all have similar color and brightness temperatures of 120–150 K.

c) *Luminosity of IRc2*

The most striking feature of the infrared spectra in Figures 3 and 4 is the 9.7 μm silicate feature in IRc2, which is an order of magnitude deeper than in BN or the other infrared peaks (cf. Rieke and Low 1973; Aitken *et al.* 1980). At 20 μm, IRc2 is a factor of 2 weaker than several of the other peaks on the map. At 8.7 μm, however, it is the second strongest source in the region, after BN. These data indicate that IRc2 is a *hot* source, which is heavily reddened at wavelengths shorter than ~10 μm.

If we define the change in dust optical depth between the center of the 9.7 μm silicate feature and the adjacent continuum as

$$\Delta\tau = \ln(S_{8\mu m}/S_{9.7\mu m}), \quad (1)$$

where S is the observed flux density, then:

$$\Delta\tau \geq 3.5 \text{ for IRc2},$$

$$\Delta\tau \sim 0.5 \text{ for BN}.$$

Because IRc2 and BN have similar color temperatures, any correction of the observed near-infrared spectrum of IRc2 must be at least $\exp(\Delta\tau_{IRc2} - \Delta\tau_{BN}) = 20$ times greater than a similar correction for BN. IRc2 has half the flux of BN at 7.9 and 12.5 μm (Figure 3; for IRc2 multiply scale by 10). Hence, the extinction correction and the expected reddening law (Becklin *et al.* 1978) imply that IRc2 is more luminous than BN. The *uncorrected* infrared spectrum of BN corresponds to a luminosity of $1.5 \times 10^3\ L_\odot$ (Becklin, Neugebauer, and Wynn-Williams 1973), almost all of which is emitted in the 5–20 μm range. Various authors have suggested models in which the *total* flux of BN is $\sim 10^4 L_\odot$ (e.g., Bedijn, Habing, and de Jong 1978; Rieke *et al.*). Corresponding to these values for BN, the luminosity of IRc2, by the above reasoning, would be $1.5 \times 10^4 - 10^5\ L_\odot$.

It is difficult to make a more precise estimate than this, particularly since the character of the silicate absorption in IRc2 and BN may be different from that in more widely distributed, "interstellar" dust. Furthermore, such a correction of the 5–20 μm infrared spectrum probably gives only a *lower limit* on the total luminosity of IRc2 because (i) the flux measured at the center of the silicate feature may be partly contributed by foreground material, so the silicate feature may be even deeper than measured; (ii) radiation transfer ef-

© American Astronomical Society • Provided by the NASA Astrophysics Data System

1981ApJ...244..869D

fects may lead to the silicate *absorption* being partially "filled in" by silicate *emission* (e.g., Kwan and Scoville 1976*a*); (iii) the contribution of radiation at wavelengths shorter than 5 μm is uncertain, particularly if the foreground extinction is $A_v \gtrsim 100$ mag; and (iv) the geometry of obscuring material is uncertain. IRc2 may thus be the most luminous object in the KL Nebula; it may account for an appreciable part of the total luminosity of $10^5\ L_\odot$ measured for KL in the far-infrared.

III. A NEW INTERPRETATION OF THE KL NEBULA

Until now, the KL Nebula has been widely referred to as a cluster of protostellar objects whose relative stages of evolution and relative luminosities were unknown. The present infrared data, combined with maser observations, now support an interpretation in which IRc2 is the main source of luminosity in the KL Nebula with a large scale outflow of matter observable in the SiO maser and thermal lines, the high velocity H_2O masers, the broad "plateau" feature in various molecular lines, and the 2 and 12.8 μm molecular hydrogen quadrupole emission.

a) Direct Evidence

The main arguments for this interpretation are:

1. The deep silicate feature suggests that IRc2 is more luminous than any other source in the KL region and contributes an appreciable part of the total luminosity of $10^5\ L_\odot$ derived from far-infrared measurements. It may therefore be a significant heating source for the dust throughout the KL Nebula.

2. The proper motions of the Orion H_2O masers measured by VLBI over a 40″ diameter region show that the "low velocity" H_2O masers are moving outward at a velocity of 18 km s^{-1} from a single source located within 5″ of IRc2. The "high velocity" H_2O masers also have a center of expansion consistent with IRc2 (Genzel *et al.* 1981).

3. The Orion "shell-type" SiO, OH, and H_2O masers, which are generally characteristic of an expanding envelope, are coincident with IRc2 (Genzel *et al.* 1979; Baud *et al.* 1980; Norris, Booth, and McLaughlin 1980; Hansen and Johnston 1981).

4. IRc2 is near the center of symmetry of the extended contours of the KL Nebula at 20 μm (Fig. 1) and is also symmetrically located between the peaks of the distribution of molecular hydrogen emission mapped by Beckwith *et al.* (1978).

b) The Mass Loss Interpretation

Figure 5 displays a variety of corroborating evidence to support the picture of exceptionally high mass loss from IRc2. The strong wind and high luminosity of IRc2 provide a natural explanation of the temperature, velocity, and density structure in the KL Nebula. The mass loss also accounts for a large fraction of the observed extinction to IRc2.

The data in Figure 5 were taken from selected radio and infrared observations. The size of the data boxes are determined by the range or uncertainty in the distance from IRc2 (horizontal boundaries of data boxes) and in the derived excitation or color temperatures, velocity spread, and H_2 number densities (vertical boundaries of the data boxes).

i) *Temperature Structure*

Since IRc2 produces maser emission in the excited *vibrational* levels of SiO, there must be regions in IRc2 at a much higher temperature than the uncorrected infrared color temperature. The VLBI data (Genzel *et al.* 1979) suggest $1000 < T_c < 3000$ K at $r \gtrsim 10^{14}$ cm. At greater radii from IRc2, the infrared color temperatures and the excitation temperatures of a variety of molecular species are consistent with radiative heating by a central energy source located within a few seconds of arc of IRc2 (Fig. 5, upper).

ii) *Velocity Structure*

Numerous molecular species in the KL Nebula display emission over a velocity range of $\Delta V \geq 36$ km s^{-1} (the "plateau" feature). The H_2O proper motion data (Genzel *et al.* 1981) suggest that there are two distinct flows, a *low velocity flow* at a constant velocity of 18 km s^{-1}, and a *high velocity flow* over the range 30–100 km s^{-1}. These two flows can also be seen in the wings of the CO plateau feature (e.g., Kuiper, Rodriguez-Kuiper, and Zuckerman 1978). The center of expansion of the

FIG. 5.—Temperature, outflow velocity, and H_2 number density vs. distance from IRc2, from radio and infrared observations. The boundaries of the data boxes correspond to the uncertainty in T, V, or n_{H_2} and to the range in distance from IRc2 over which the species is observed. *Upper Diagram*: The upper and lower diagonals correspond to radiative heating of optically thin dust with absorption efficiency $Q_\lambda \propto \lambda^{-1}$ and $L = 10^5$ and $10^4\ L_\odot$, respectively. The lower diagonal also fits optically thick dust with $L = 10^5\ L_\odot$. *Central Diagram*: The dashed lines correspond to the 18 km s^{-1} flow and to the boundaries of the H_2O high velocity flow. *Lower Diagram*: The diagonal line corresponds to a mass loss rate $\dot{M} = 10^{-3}\ M_\odot$ yr^{-1}, $V_{\rm wind} = 18$ km s^{-1} and $\rho \propto r^{-2}$. References: SiO $V = 1, 2$ masers (Genzel *et al.* 1979; Baud *et al.* 1980), H_2O "shell" masers (Genzel *et al.* 1979), IRc2–4 color temperatures (this paper), HC_3N (Clark *et al.* 1976; Deguchi *et al.* 1979), H_2O low and high velocity masers (Genzel and Downes 1977; Genzel *et al.* 1978; Genzel *et al.* 1981), SiO $V = 0$ emission (Genzel *et al.* 1980; Wright *et al.* 1980), SO_2 (Wannier *et al.* 1980), NH_3 (Wilson, Downes, and Bieging 1979; Morris, Palmer, and Zuckerman 1980), CO 1–0 (Kwan and Scoville 1976*b*; Kuiper, Rodriguez-Kuiper, and Zuckerman 1978), CO 2–1 (Wannier *et al.* 1980), CO 3–2 (Phillips *et al.* 1977), CH_3OH (Matsakis *et al.* 1980), H_2 (Beckwith *et al.* 1978; Nadeau and Geballe 1979), 20–120 μm (Erickson *et al.* 1977; Werner *et al.* 1976), mm continuum (Westbrook *et al.* 1976).

© American Astronomical Society • Provided by the NASA Astrophysics Data System

1981ApJ...244..869D

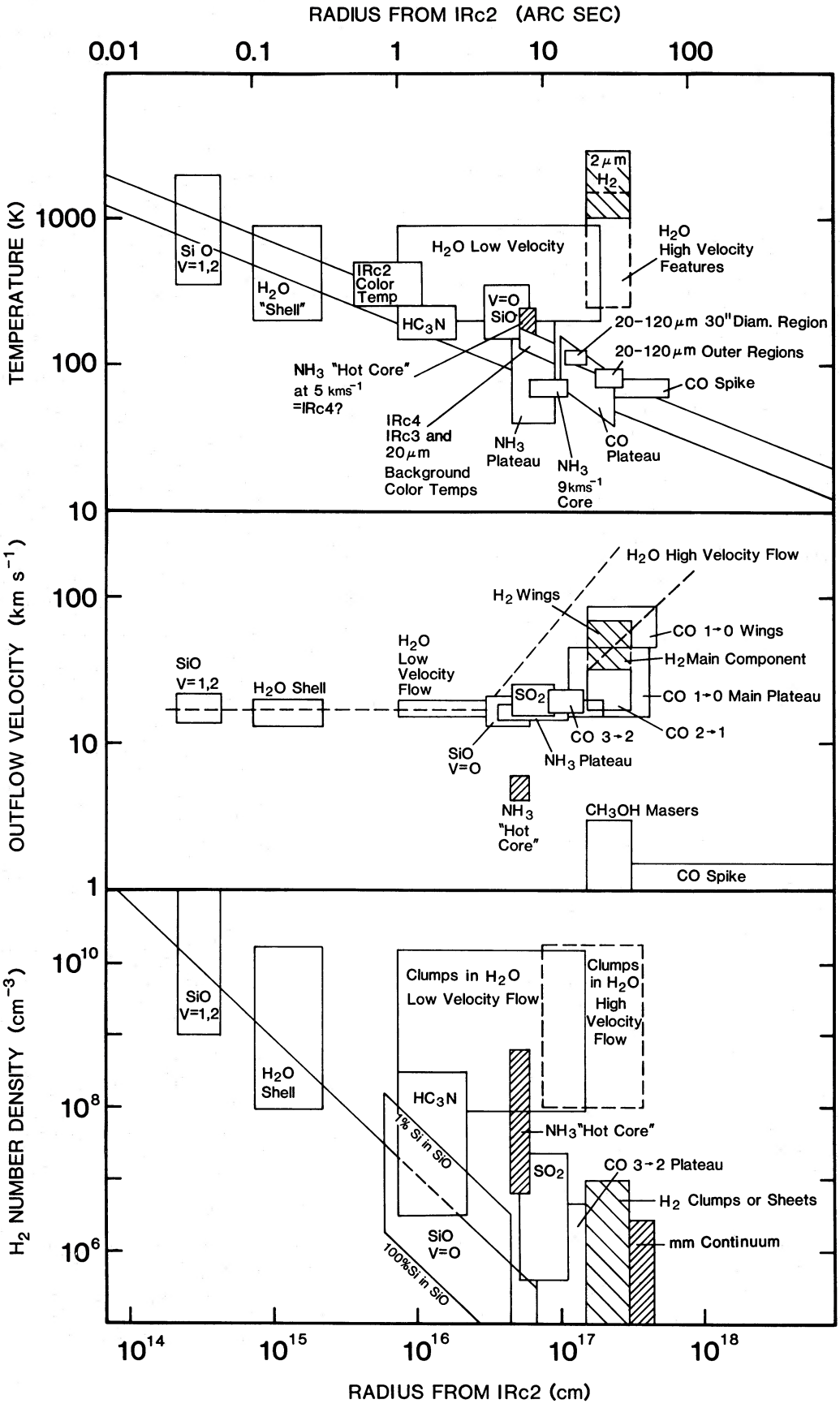

FIG. 5

© American Astronomical Society • Provided by the NASA Astrophysics Data System

1981ApJ...244..869D

18 km s^{-1} plateau emission is best defined in the ground vibrational state of SiO, and agrees with IRc2 to within $\pm 1''$ (Wright *et al.* 1980; Genzel *et al.* 1980). This is believed to be *thermal* SiO emission in the 18 km s^{-1} flow, with an angular radius $\sim 5''$ about IRc2.

Though less well defined than the thermal SiO, the position of the "plateau" emission of J=3–2 CO, NH_3, and HCN is definitely south of BN (Phillips *et al.* 1977; Wilson, Downes, and Bieging 1979; Rydbeck *et al.* 1980) and is also consistent with outflow from IRc2. Although the "plateau" emission in the $J=1\rightarrow 0$ line of CO is even more spatially extended than in some other molecules, its centroid may also be at IRc2 (Scoville 1980).

An important result is that the velocity spread of various molecular lines shows that the 18 km s^{-1} flow velocity is constant from $r=10^{14}$ to 10^{17} cm from IRc2 (Fig. 5, center). This indicates a *continuous*, steady outflow from IRc2. Nadeau and Geballe (1979) argue that the infrared H_2 emission could also be occurring over a continuous, filled region and not in a thin shell. Thus, the earlier proposal by Kwan and Scoville (1976*b*), that the flow originated in a supernova explosion, is no longer required. The proper motions of the high-velocity H_2O masers indicate that the high velocity flow may also come from IRc2. Both the low and high velocity flows seem to end at $\sim 10^{17}$ cm from IRc2, which implies a time scale of 10^3–10^4 years (Appendix 1).

iii) *Density Structure*

The estimates of H_2 number density in the 18 km s^{-1} outflow (Fig. 5, lower) are very roughly consistent with $n_{H_2} \propto r^{-2}$, from $r=10^{14}$ to 10^{17} cm, as would be expected from constant mass loss. On a larger scale than shown in the figure, the observations of millimeter continuum emission (Westbrook *et al.* 1976) and CS and other molecular lines (Goldsmith *et al.* 1980) suggest that even beyond the mass-loss region, n_{H_2} continues to decrease as r^{-2} from $r=10^{17}$ to 10^{18} cm as well, at least in the east-west direction. The rate of mass loss consistent with the data in Figure 5 is 10^{-4}–10^{-3} $M_\odot$ yr^{-1} in the 18 km s^{-1} flow. The diagonal line in Figure 5 is for the latter value. The rate of mass loss in the high velocity flow, as estimated from the wings of the CO lines, is about an order of magnitude less (Genzel *et al.* 1981). Thus the momentum transport $\dot{M}v$, in the low and high velocity flows is about the same, while the mechanical power, $\dot{M}v^2/2$, is an order of magnitude greater in the high velocity flow, namely, 10^2–10^3 $L_\odot$. This may account for the luminosity of $\sim 10^3$ $L_\odot$ radiated in the molecular hydrogen lines (Beckwith *et al.* 1978).

IV. NATURE OF THE COMPACT INFRARED SOURCES IN THE KL NEBULA

a) *Is IRc2 a Young Star?*

IRc2 is so far the only SiO maser source in a region of star formation. The double-peaked SiO maser profile, the low outflow velocity of 18 km s^{-1}, and the luminosity of 10^4–10^5 $L_\odot$ are very similar to the properties of evolved M giants and supergiants (Snyder *et al.* 1978). Despite this evidence, the following reasoning suggests that IRc2 is a young star rather than an evolved object.

i) *At Density Maximum of Orion Molecular Cloud*

IRc2 is located in the densest part of an extended molecular cloud. IRc2 lies within $\pm 5''$ of the density maximum defined by sub-mm maps (Westbrook *et al.* 1976; Werner *et al.* 1976, 1977; Keene, Hildebrand, and Whitcomb 1981). Westbrook *et al.* estimate a mass of 200 $M_\odot$ for the central 1′ region, so it is unlikely that the density maximum has been produced by the mass loss from IRc2.

ii) *Proximity to the BN Object*

IRc2 is located very near to the BN object which has recently been interpreted to be a young, massive star (§ IV*b*). The CO absorption-line system seen at 4.6 μm by Hall *et al.* (1978), blueshifted relative to $V_{LSR}=9$ km s^{-1}, can be interpreted as the outflow from IRc2 seen in absorption against BN. That is, IRc2 is not only close to BN on the sky but is actually *physically* nearby. Arguments i) and ii) make it most unlikely that IRc2 is simply a luminous, evolved field star well behind the Orion molecular cloud.

iii) *Similarity to Other Compact Objects in Star-Forming Regions*

IRc2's deep silicate absorption, low and high velocity H_2O emission, and lack of radio continuum emission (<3 mJy at 6 cm; M. Simon, private communication) are similar to the properties of many other radio-quiet, compact infrared sources in the vicinity of young O associations, compact H II regions, and other tracers of recent star formation. The high velocity H_2O masers seem to be especially correlated with young objects. So far, no high velocity H_2O has been seen near evolved stars, such as the known M supergiants.

iv) *No Evidence for Extensive "Clearing"*

If IRc2 had been a 10^5 $L_\odot$ O star which has now evolved off the main sequence, it would have had 5×10^6 years to clear out the surrounding molecular cloud by radiation pressure, stellar winds, and expansion of its H II region. Familiar examples are the O

© American Astronomical Society • Provided by the NASA Astrophysics Data System

1981ApJ...244..869D

stars in W3 A and the Orion Trapezium, both of which have cleared out an H II region to $r=10^{18}$ cm and reduced the density to $n_e \sim 10^3-10^4$ cm^{-3} (Wynn-Williams 1971; Menon 1961).

By contrast, the 18 km s^{-1} flow from IRc2 decelerates to zero velocity at $r\sim 2\times 10^{17}$ cm (Fig. 5), where the density of the medium is $\sim 10^5-10^6$ cm^{-3}. Beyond this radius, quiescent, ambient gas dominates and produces the narrow-line "spike" feature at $V_{LSR}\sim 9$ km s^{-1} seen in many molecular lines. Hence, there has not yet been the extensive "clearing" which one would expect during the main sequence lifetime of an O star. The many infrared objects, such as IRc3–8 in the vicinity of IRc2, are also evidence against such clearing.

Furthermore, the far-infrared spectrum of the Orion KL Nebula is quite different from that of objects like IRC+10216 (Campbell *et al.* 1976), VY CMa (see the compilation by Schwartz 1975), or η Car (Harvey, Hoffmann, and Campbell 1978). Whereas these objects have "hot" spectra peaking between 5 and 20 μm, the KL Nebula has a much greater far-infrared flux. IRc2 may thus have a much larger amount of surrounding dust, or a much greater mass loss, than these other objects.

v) *Differences from Evolved M Supergiants*

1. The mass loss of $10^{-4}-10^{-3}\ M_\odot$ yr^{-1} in the 18 km s^{-1} flow, estimated from the thermal lines of SiO and CO, is 2 orders of magnitude larger than the mass-loss rates derived for M supergiants by Morris *et al.* (1979) and Gehrz and Woolf (1971).

2. The pattern of radio lines in IRc2 is different from that in M supergiants. There are no strong, unpolarized OH lines at 1612 MHz as in NML Cyg or VY CMa.

3. The absence of SiO masers in most young infrared objects may simply indicate a sensitive dependence of the SiO masers on temperature, $\dot{M}$, turbulence, location of the grain condensation radius, velocity gradient, etc., rather than on whether the star is an evolved object or not. The high mass loss in IRc2 may cause the SiO masers to see a "false photosphere" with $T_c \lesssim 3000$ K, similar to the environment near evolved stars.

b) *The BN Object*

Although there were numerous models in the earlier literature which treated BN as an accreting protostar, one current view is that BN is a young, hot star which is losing mass and is therefore surrounded by a dust envelope. In order of increasing radius from BN, the picture is:

1. $r=10^{11}-10^{12}$ cm: This is the photosphere and possibly the ionized envelope of the star. There are two interpretations of the Brackett and Pfund lines seen from BN: (a) the lines are photospheric, from a star with surface temperature $5000<T<20{,}000$ K; (b) the lines come from a small H II region—the ionized envelope of the star—in which case the intensity of the Brackett lines and the Bα/Bγ and Pfγ/Bγ ratios can be interpreted in terms of ionized gas around a B0 to B2 exciting star (Grasdalen 1976; Hall *et al.* 1978). The hydrogen lines are redshifted by 12.5 km s^{-1} relative to the Orion molecular cloud, or by 16 km s^{-1} relative to IRc2. Hall *et al.* propose that the redshift is due either to scattering off dust or absorption of the blue wing of the Brackett lines by hydrogen in an expanding envelope. Alternatively, it could be the velocity of BN itself. The Brackett α and γ profiles have high-velocity ($\Delta v\sim 150$ km s^{-1}) wings characteristic of early-type stars with stellar winds (Hall *et al.* 1978; Scoville 1981).

2. $r=10^{12}-10^{13}$ cm: Probable location of the 2.3 μm CO band emission discovered by Scoville *et al.* (1979), who propose that the region has $n_{H_2}>10^{10}$ cm^{-3} and $T\sim 3000-5000$ K. Another, separate CO emission-line system has also been reported (see Scoville 1980).

3. $r=3\times 10^{14}$ cm: Location of circumstellar dust at $T_c\sim 500$ K, from measurements of the 0".1 size of BN at 4.8 and 3.5 μm (Chelli, Lena, and Sibille 1979; Foy *et al.* 1979).

4. $r\sim 10^{16}-10^{17}$ cm: Probable location of the broad ($\Delta V=40$ km s^{-1}) 4.6 μm CO absorption seen toward BN at $V_{LSR}=-16$ km s^{-1}. Hall *et al.* (1978) suggest that this cool material ($T_{rot}\gtrsim 100$ K) is being driven outward by BN. In our opinion, it is also possible that this is actually the wind from IRc2, seen in absorption against BN.

5. $r=10^{17}-10^{18}$ cm: Location of the narrow-line ($\Delta V=6$ km s^{-1}) 4.6 μm CO absorption seen toward BN at $V_{LSR}=9$ km s^{-1} (Hall *et al.* 1978). This is probably the stationary, cool ($T_{rot}\sim 100$ K) gas of the Orion molecular cloud, exterior to the IRc2 wind region.

From the relative depth of the silicate feature, we estimate that the luminosity of BN is roughly a tenth that of IRc2. In all other respects, BN appears to be losing mass in the same manner as IRc2. This would account for the circumstellar dust shell of BN and provide a natural explanation for its infrared spectrum. The lower luminosity and lower rate of mass loss from BN would imply lower temperatures and shorter maser gain paths than in IRc2 and account for the lack of maser emission from BN.

c) *Other Infrared Sources in the KL Nebula*

The compact sources IRc3–7 in the central region of the KL Nebula appear prominently on the 20 μm map but not on maps at shorter wavelengths. IRc3, IRc4,

© American Astronomical Society • Provided by the NASA Astrophysics Data System

1981ApJ...244..869D

and IRc5 are extended (3″–4″) objects with color and brightness temperatures $T_c \sim T_b \sim 100$–150 K, and hence are cooler sources than IRc2 or BN.

Zuckerman, Palmer, and Morris (1980) propose that IRc4 is the "NH_3 hot core" at $V_{LSR} \sim 5$ km s^{-1}. IRc4 would then be nearly stationary relative to IRc2, which has a velocity of 5.5 km s^{-1}, the centroid of the SiO masers. IRc4 and possibly other peaks like IRc3 may be dense remnants of the original fragmentation of the center of the Orion molecular cloud. The 18 km s^{-1} flow from IRc2 would stream through the central region of the KL Nebula, possibly creating the H_2O masers near IRc4 and IRc5. The objects IRc3–7 may be objects in an earlier stage of evolution than BN or IRc2 with luminosity sources of their own. Alternatively, these objects might simply be high density condensations with near-infrared optical depths > 1 which are heated by the radiation and outflow from IRc2.

V. INFRARED EMISSION AND MASERS

a) Comparison of Infrared Sources and H_2O *Masers*

Figure 6 shows the positions of H_2O masers relative to the 20 μm contours. The main results are:

1. IRc2 coincides with H_2O masers, as well as with OH and SiO masers.

2. IRc4 is associated with a strong cluster of H_2O masers (the maser group called "H_2O Source A" by Genzel and Downes 1977).

3. IRc5 (our revised infrared position) is near to the H_2O maser group (called "Source B" by Genzel and Downes 1977).

4. There is a bulge in the infrared contours near the H_2O low and high velocity masers at $05^h32^m46^s.3$, $-05°24'30''$.

5. IRc9 agrees in position with a low velocity H_2O maser at 6.2 km s^{-1} and is near a high velocity maser group at 60–70 km s^{-1}.

6. The H_2O maser at 8.1 km s^{-1} flared up in 1979 October to become the brightest maser in the sky with a line flux density $> 10^6$ Jy (Abraham, Opher, and Raffaelli 1979). The maser is located on the extended 20 μm contours west of IRc4; there is no compact infrared source at this position. The maser radiation may be highly beamed with the only physical change in the source being a shift in the beam direction from its preflare state.

7. No masers are associated with the BN object.

8. There is no infrared counterpart of the H_2O maser group at $05^h32^m47^s.6$, $-05°24'09''$, and $V_{LSR} \sim 9$–12 km s^{-1}. For many years, this group contained the strongest maser line in Orion (10^4 Jy). The absence of 20 μm emission in the northeastern portion of the map may indicate a lack of warm dust or unusually high foreground extinction.

9. Most of the high velocity H_2O masers have no infrared counterparts.

10. The H_2O masers and the 20 μm infrared peaks do not coincide with the peaks of the 2 μm quadrupole line emission of molecular hydrogen (e.g., Beckwith *et al.* 1978), as may be seen in Figure 6. There are H_2O masers near a peak in the H_2 emission near IRc9, and another group of H_2O sources near the H_2 peak to the southwest of IRc3. It is a curious coincidence that the H_2O masers at 60–70 km s^{-1}, the most long-lived of all the high velocity H_2O masers in observations over 1976 through 1979, have been those nearest the main peaks of the molecular hydrogen emission (see the lower left and upper right corners of Fig. 6).

b) Three Types of H_2O *Masers*

Comparison of the H_2O data and infrared maps suggests that there are three types of H_2O masers in the KL Nebula. (For a more general discussion of these types see Genzel *et al.* 1981; here we only remark on their relation to the infrared sources.)

i) *The Masers Directly Associated with IRc2*

The "shell-type" features are similar to the double-peaked maser profiles observed in the expanding circumstellar envelopes of evolved stars. The H_2O masers in IRc2 are less time-variable and ~ 10 times larger in apparent angular size than all the other H_2O masers in Orion (Genzel *et al.* 1979). From the size of the cluster of H_2O "spots" on VLBI maps, these masers are located $\sim 10^{15}$ cm from IRc2. At this radius, the radiation in the envelope should have a color temperature of 500–1000 K and a maximum flux near the 2.7 and 6 μm vibrational bands of H_2O. The H_2O "shell" masers may be radiatively pumped by the near-infrared radiation and may be formed in favorable gain paths at "stationary" locations from IRc2.

ii) *Low-Velocity* H_2O *Masers throughout the KL Nebula*

The other H_2O masers in Orion are qualitatively different from the "shell" masers in IRc2. As well as being smaller, more variable, and often more intense than the IRc2 masers, nearly all of these other H_2O masers have proper motions or radial velocities which may be interpreted as motion away from IRc2 (Genzel *et al.* 1981). These masers may be formed from dynamical instabilities as the 18 km s^{-1} wind encounters "stationary" clouds in the KL Nebula. This process might explain the good correlation of low velocity H_2O masers with the 20 μm condensations. The pumping of these masers is probably collisional or radiative through the far-infrared transitions of H_2O.

© American Astronomical Society • Provided by the NASA Astrophysics Data System

1981ApJ...244..869D

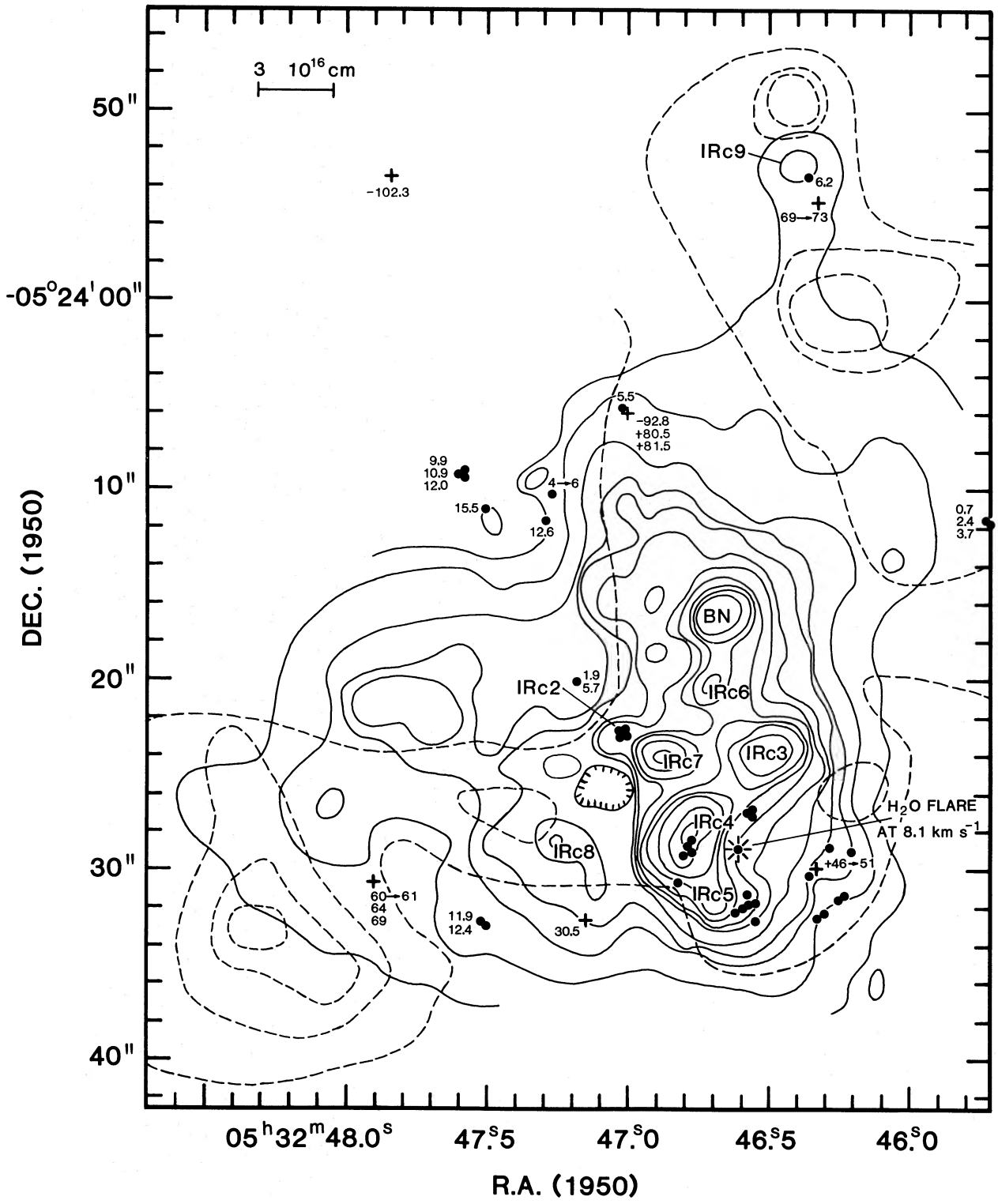

FIG. 6.—Locations of H_2O masers in the KL Nebula. *Labels* are LSR radial velocities in km s^{-1}. VLBI positions of low velocity H_2O masers are shown as *black dots* (Genzel *et al.* 1978, 1981), superposed on the 20 μm infrared contours from Fig. 1. Crosses show the positions of weak, high velocity H_2O masers (Genzel and Downes 1977; Genzel *et al.* 1981). The H_2O maser at 8.1 km s^{-1} flared in late 1979 to become the brightest maser in the sky, with a flux $> 10^6$ Jy. *Dashed contours* are those of the $v = 1-0$ S(1) transition of molecular hydrogen (Beckwith *et al.* 1978). Linear scale is for an assumed distance of 500 pc.

© American Astronomical Society • Provided by the NASA Astrophysics Data System

1981ApJ...244..869D

iii) *High-Velocity* H_2O *Masers*

The high velocity H_2O masers are of low intensity, highly variable, and usually at the largest radii from IRc2 of all the masers. They are not correlated with infrared peaks and are likely to be collisionally pumped. The high velocity H_2O masers (Fig. 6, $|V_{LSR}|>30$ km s^{-1}), along with the broad wings of the H_2 and CO emission, show that there is a second, "high velocity" outflow, in addition to the steady, 18 km s^{-1} outflow. The high velocities may occur if the wind is time variable, if the star throws off material in bursts from time to time, or if some other agent, such as radiation pressure on dust can drive the material to higher speeds. The latter process would be easier in "rarefied" regions which have density gradients steeper than $\rho \propto r^{-2}$.

VI. THE ENVIRONMENT OF NEWLY FORMED, MASSIVE STARS

a) *IRc2 as a Prototype*

In this paper we have argued from the infrared and maser results that IRc2 may be a young object rather than an evolved star. If IRc2 produces most of the 10^5 $L_\odot$ luminosity of KL, it could contain something resembling a B0 to O7 star, with a mass-loss rate of $10^{-4}-10^{-3}$ $M_\odot$ yr^{-1}. IRc2 is probably not unique. The observations of low and high velocity emission in many H_2O masers throughout the Galaxy suggest that Orion-KL might be typical of regions of active star formation. The 2 μm H_2 emission in DR 21, W3(OH), and other young regions (Fischer, Righini-Cohen, and Simon 1980; Gautier 1980), as well as the broad CO wings towards S140 (R. Plambeck, private communication), L1551 (Snell, Loren, and Plambeck 1980), and Cep A (Rodriguez, Ho, and Moran 1980) also support the idea that the IRc2-type outflow is a common phenomenon in star-forming regions. The reason why more examples of molecular "plateau" features and H_2 emission have not yet been found is probably the small solid angle of the flow region in distant sources. In W51, for example, the 40″ CO "plateau" region in Orion would subtend only 3″, which would reduce the CO line temperature in the beam of the Kitt Peak 11 m telescope by a factor of several hundred. Such flows will doubtlessly be found in other young regions as detector sensitivities improve and as larger millimeter telescopes come into operation.

b) *Structure of the Region*

We now use the example of IRc2 and the KL Nebula to describe the possible structure, in order of increasing radius, from a newly formed star in an active state of mass loss:

1. $r=10^{11}-10^{12}$ cm: The radius of a B0 to O7 star of $L=10^4-10^5$ $L_\odot$ and mass loss $\dot{M}\sim 10^{-4}-10^{-3}$ $M_\odot$ yr^{-1} at a velocity of $\sim$18 km s^{-1}. In addition to this low velocity outflow, there may also be a (time variable?) high velocity outflow at a level of $\dot{M}\sim 10^{-5}$ $M_\odot$ yr^{-1} and $V=30-100$ km s^{-1}. There may be a small ionized region a few stellar radii in size. Beyond this, the *wind prevents the formation of an* H II *region*, since the recombination time is much shorter than the dynamical time scale of the flow. The critical mass-loss rate for suppressing a compact H II region is

$$\dot{M}_{crit}=2(2\pi)^{1/2}\mu m_H v_{wind}(N_{UV}R_c/\alpha)^{1/2}, \quad (2)$$

for a wind with $\rho \propto r^{-2}$ (see, e.g., Wright and Barlow 1975), and for μ the mean molecular weight of the gas, m_H the hydrogen mass, N_{UV} the number of ionizing photons, R_c the radius at the origin of the flow, and α the recombination coefficient. For $\dot{M}<\dot{M}_{crit}$, the entire flow can be ionized, and for $\dot{M}>\dot{M}_{crit}$, the ionized mass is confined to a very small radius close to that of the star. If, for example, IRc2 had an *ultraviolet* luminosity of 10^5 $L_\odot$, as in an O7 star, then $\dot{M}_{crit}\sim 10^{-6}$ $M_\odot$ yr^{-1}, much less than the observed mass loss, so the 18 km s^{-1} outflow from IRc2 would be mainly neutral.

This argument also holds for the origin of the high velocity flow ($\dot{M}\sim 10^{-5}$ $M_\odot$ yr^{-1}). It is more likely that the high velocity flow is associated with IRc2 than with BN, since the latter source may have a small H II region, as indicated by its Brackett and Pfund lines. Hence, the rate of mass loss from BN is probably less than $\dot{M}_{crit}\sim 10^{-6}$ $M_\odot$ yr^{-1}, that is, insufficient to account for the high velocity flow in the KL Nebula.

2. $r=10^{13}-10^{14}$ cm: In this range, the temperature of the flow may fall to $\sim 10^3$ K (Fig. 5), whereupon grains may condense and molecules form. A dust condensation temperature of $\sim$1000 K has been deduced for a variety of objects including novae (e.g., Gehrz *et al.* 1980) and carbon-rich circumstellar shells (Ney and Merrill 1977). In this picture, *the outflow has produced the grains, and not vice versa*. Similar conclusions have been reached from model atmosphere calculations (Fix and Alexander 1974), from lunar occultation measurements of IRC+10011 (Zappala *et al.* 1975), and from studies of late-type stars (Boesgaard and Hagen 1979). Once formed, the grains may contribute to further acceleration of the flow as they absorb radiation from the star.

3. $r=10^{14}-2\times 10^{16}$ cm: This is the location of unimpeded flow, at 18 km s^{-1} in the case of IRc2. Proceeding out in radius, one finds the double-peaked "shell-type" masers of SiO at a few times 10^{14} cm, H_2O at $\sim 10^{15}$ cm, and OH at $\sim 10^{16}$ cm.

4. $r=10^{16}-10^{17}$ cm: This range is likely to contain "stationary" objects such as fragments remaining from the original contraction of the molecular cloud. This is one of the chief differences between mass loss in a region of star formation and that in an isolated, evolved star. The former type of flow will encounter a very

© American Astronomical Society • Provided by the NASA Astrophysics Data System

1981ApJ...244..869D

nonuniform medium, with a mixture of regions of lower and higher density. In Orion-KL this medium contains BN, the compact infrared sources IRc3–7, and clumps of hot gas such as the "hot core" in ammonia lines (e.g., Morris, Palmer, and Zuckerman 1980).

The flow phenomena will thus be a mixture of the unhindered flow and interactions of the wind with the ambient matter. In Orion-KL, the evidence for such interactions may be (i) the low and high velocity H_2O masers, which might form at dynamically unstable interfaces of the wind and the surrounding material; (ii) the radial velocity centroid of the low velocity of H_2O masers. This centroid differs by 4 km s^{-1} from the velocity of IRc2, as would be expected from drag between the flow and stationary material of the Orion molecular cloud (Genzel *et al.* 1981). (iii) The appearance of maxima in the H_2 emission at large radii from IRc2 at the edges of the 20 μm distribution, which may be related to (iv) the apparent deceleration of the outflow and disappearance of molecular-line "plateau" features at radii $\sim 10^{17}$ cm (see Appendix 1).

5. $r = 10^{17} - 4 \times 10^{17}$ cm: In Orion-KL this is the central "core" of the Orion molecular cloud, as shown on numerous molecular-line maps of the narrow "spike" component at $V_{LSR} \sim 9$ km s^{-1} and on far-infrared maps (Werner *et al.* 1977). The maps at a wavelength of 1 mm show that this core is an actual maximum of density.

6. $r = 4 \times 10^{17} - 2 \times 10^{18}$ cm: In Orion this is the extended north-south ridge of the molecular cloud.

c) *What Causes the Mass Loss?*

Numerous mechanisms have been proposed for mass loss in stars, including a pulsational instability in young, massive stars (Hoyle, Solomon, and Woolf 1973), rotationally induced mass loss (e.g., Larson 1980), ion-line driven winds (Castor, Abbott, and Klein 1975), acoustic flux mechanisms (Fusi-Pecci and Renzini 1975; Martens 1979), dust-driven winds (e.g., Menietti and Fix 1978; Phillips 1979), loss of angular momentum by magnetic effects (e.g., Lüst and Schlüter 1955; Ebert, von Hoerner, and Témesvary 1960), and wind-driven turbulence in a circumstellar disk (Elmegreen 1978), to mention but a few. In the last cited mechanism, most of the mass loss comes from the disk rather than the star itself.

The wind from IRc2 is unlikely to be a radiation-driven wind of the type described for O stars by Castor *et al.* The wind from IRc2 is of low velocity and probably *neutral* from $r = 10^{14} - 10^{17}$ cm, and is apparently several orders of magnitude stronger than would be predicted by the line-driven wind theory; for a star of $L = 10^5\ L_\odot$, the formulae of Castor, McCray, and Weaver (1975) predict $\dot{M} < 10^{-6}\ M_\odot\ yr^{-1}$.

We also note that the IRc2 phenomenon has nothing to do with protostar models in which a newly formed star reverses the accretion flow and forms an outward-moving dust front by virtue of its radiation pressure (e.g., Kahn 1974; Yorke and Krügel 1977). If IRc2 is a young object, then its wind completely overwhelms all other structures ("cocoons," "dust fronts") which would form by the interaction of radiation pressure and accretion alone.

We suggest that the wind is related to a previously neglected process in the internal structure of the star itself, that it strongly influences the lifetime of the maser phase as well as the eventual appearance and lifetime of a compact H II region, and that it is a dominating factor in the appearance of newly formed, massive stars.

D. D. wishes to thank J. T. Jefferies for his generous hospitality at the University of Hawaii. C. G. W.-W. and D. D. acknowledge the support of NATO research grant No. 1909. We are grateful to the staff of the IRTF for assistance, especially Ron Koehler for help with the observations. This research was also supported by NASA contract NASW-3159 and NSF grant AST 78-26028.

APPENDIX 1

DECELERATION AND AGE OF THE FLOW

The motion of the wind is complicated by the inhomogeneous distribution of clouds in the KL Nebula. For $10^{16} < r < 10^{17}$ cm, the flow may encounter high-density cloudlets in some directions (IRc3–7) and rarefactions in other sectors. The following approximation gives a rough idea of the dynamics.

Assume that there is unimpeded flow at rate $\dot{M}_\odot$ and velocity v_0 into a sector of solid angle Ω. Beyond some radius r_0 from IRc2, the flow encounters a medium of density

$$\rho(r) = \rho_0 (r_0/r)^n. \quad \text{(A1)}$$

© American Astronomical Society • Provided by the NASA Astrophysics Data System

1981ApJ...244..869D

The mass swept up by the flow in this sector will be

$$M(r)=\Omega\int_{r_0}^{r}R^2\rho(R)\,dR. \tag{A2}$$

In the limit where the swept-up mass exceeds that of the original ejecta, the equation of motion is

$$\frac{d}{dt}[M(r)v(r)]=\dot{M}_\odot v_0\frac{\Omega}{4\pi}. \tag{A3}$$

(For IRc2 wind pressure exceeds radiation pressure on dust if $\dot{M}_\odot > 10^{-4}\,M_\odot\ \mathrm{yr}^{-1}$.) The solution for $n\leq 2$ and $r>r_0$ is:

$$r=At^\beta, \qquad v=Br^\alpha, \tag{A4}$$

where $\beta=2/(4-n)$, $\alpha=(n-2)/2$, $B=A^{1/\beta}$, and

$$A=\left[\frac{(4-n)(3-n)\dot{M}_\odot v_0}{8\pi r_0^n\rho_0}\right]^{1/(4-n)}. \tag{A5}$$

Note that the often cited relation, $r\propto t^{3/5}$ (e.g., Avedisova 1971; Castor, McCray, and Weaver 1975) probably does not apply here, since (i) the wind from IRc2 appears to be cool and neutral from $r=10^{14}-10^{17}$ cm without an adiabatic, ionized, "shocked wind zone," and (ii) the wind moves into a nonuniform medium.

AGE OF THE FLOW

Beyond $r=10^{17}$ cm, the flow may be decelerated by the surrounding Orion molecular cloud. Figure 5 (center) indicates that the 18 km s^{-1} flow velocity can be measured only to a radius of several 10^{17} cm from IRc2. Slightly beyond this radius, to the northeast and southwest of the KL Nebula, the 2 μm H_2 emission reaches its maximum intensity. If the flow is stopped near these locations by large, constant-density blobs in OMC-1, then, from equations (A4) and (A5), the age of the flow would be

$$t=\left(2.09\rho_0/\dot{M}_\odot v_0\right)^{1/2}r^2. \tag{A6}$$

If, for example, there are blobs of $n_{H_2}\sim 10^5$ cm^{-3} at $r\sim(2-3)\ 10^{17}$ cm, the distance of the H_2 emission regions from IRc2, then a wind with $\dot{M}_\odot\sim 10^{-4}\ M_\odot$ yr^{-1}, $v_0=18$ km s^{-1}, will have an age $t\sim 10^4$ yr. A *lower limit* on the age of the wind is simply $t=r/v=10^{17}$ cm per 18 km s^{-1}, which is $\sim 10^3$ yr. In this *minimum* interval, IRc2 would have lost 0.1–1 $M_\odot$.

REFERENCES

Abraham, Z., Opher, R., and Raffaelli, J. C. 1979, *IAU Circ.*, No. 3415.
Aitken, D. K., Roche, P. F., Spenser, P. M., and Jones, B. 1980, *M.N.R.A.S.*, in press.
Avedisova, V. S. 1971, *Astr. Zh.*, **48**, 894 (1972, *Soviet Astr.—AJ*, **15**, 708).
Baud, B., Bieging, J. H., Plambeck, R., Thornton, D., Welch, W. J., and Wright, M. 1980, *IAU Symposium* 87, *Interstellar Molecules*, ed. B. Andrew (Dordrecht: Reidel), in press.
Becklin, E. E., Matthews, K., Neugebauer, G., and Willner, S. P. 1978, *Ap. J.*, **220**, 831.
Becklin, E. E., and Neugebauer, G. 1968, in *Interstellar Ionized Hydrogen*, ed. Y. Terzian (New York: Benjamin), p. 1.
Becklin, E. E., Neugebauer, G., and Wynn-Williams, C. G. 1973, *Ap. J. (Letters)*, **182**, L7.
Beckwith, S., Persson, S. E., Neugebauer, G., and Becklin, E. E. 1978, *Ap. J.*, **223**, 464.
Bedijn, P. J., Habing, H. J., and de Jong, T. 1978, *Astr. Ap.*, **69**, 73.
Boesgaard, A. M., and Hagen, W. 1979, *Ap. J.*, **231**, 128.
Campbell, M. F. *et al.* 1976, *Ap. J.*, **208**, 396.
Castor, J. I., Abbott, D. C., and Klein, R. I. 1975, *Ap. J.*, **195**, 157.
Castor, J., McCray, R., and Weaver, R. 1975, *Ap. J. (Letters)*, **200**, L107.
Chelli, A., Lena, P., and Sibille, F. 1979, *Nature*, **278**, 143.
Clark, F. O., Brown, R. D., Godfrey, P. D., Storey, J. W. V., and Johnson, D. R. 1976, *Ap. J. (Letters)*, **210**, L139.
Deguchi, S., Nakada, Y., Onaka, T., and Uyemura, M. 1979, *Pub. Astr. Soc. Japan*, **31**, 105.
Ebert, R., von Hoerner, S., and Temesvary, S. 1960, *Die Entstehung von Sternen* (Hamburg: Springer).
Elmegreen, B. G. 1978, *Moon and Planets*, **19**, 261.
Erickson, E. F., Strecker, D. W., Simpson, J. P., Goorvitch, D., Augason, G. C., Scargle, J. D., Caroff, L. J., and Witteborn, F. C. 1977, *Ap. J.*, **212**, 696.
Fischer, J., Righini-Cohen, G., and Simon, M. 1980, *Ap. J. (Letters)*, **238**, L155.
Fix, J. D., and Alexander, D. R. 1974, *Ap. J. (Letters)*, **188**, L91.
Foy, R., Chelli, A., Sibille, F., and Lena, P. 1979, *Astr. Ap.*, **79**, L5.
Fusi-Pecci, F., and Renzini, A. 1975, *Astr. Ap.*, **39**, 413.
Gautier, T. N. 1980, *Bull. AAS*, **11**, 439.
Gehrz, R. D., Hackwell, J. A., Grasdalen, G. L., Ney, E. P., Neugebauer, G., and Sellgren, K. 1980, *Ap. J.*, **239**, 570.

© American Astronomical Society • Provided by the NASA Astrophysics Data System

1981ApJ...244..869D

Gehrz, R. D., and Woolf, N. J. 1971, *Ap. J.*, **165**, 285.
Genzel, R., and Downes, D. 1977, *Astr. Ap.*, **61**, 117.
Genzel, R. *et al.* 1978, *Astr. Ap.*, **66**, 13.
Genzel, R., Downes, D., Schwartz, P. R., Spencer, J. H., Pankonin, V., and Baars, J. W. M. 1980, *Ap. J.*, **239**, 519.
Genzel, R., Moran, J. M., Lane, A. P., Predmore, C. R., Ho, P. T. P., Hansen, S. S., and Reid, M. J. 1979, *Ap. J.* (*Letters*), **231**, L73.
Genzel, R., Reid, M., Moran, J. M., and Downes, D. 1981, *Ap. J.*, **244**, 884.
Goldsmith, P. F., Langer, W. D., Schloerb, F. P., and Scoville, N. Z. 1980, *Ap. J.*, **240**, 524.
Grasdalen, G. L. 1976, *Ap. J.* (*Letters*), **205**, L83.
Grasdalen, G. L., Herzog, A. D., Hackwell, J. A., and Gehrz, R. D. 1980, *Bull. AAS*, **11**, 712.
Hall, D. B., Kleinmann, S. G., Ridgway, S. T., and Gillett, F. C. 1978, *Ap. J.* (*Letters*), **223**, L47.
Hansen, S. S., and Johnston, K. J. 1981, in preparation.
Harvey, P. M., Hoffmann, W. F., and Campbell, M. F. 1978, *Astr. Ap.*, **70**, 165.
Hoyle, F., Solomon, P. M., and Woolf, N. J. 1973, *Ap. J.* (*Letters*), **185**, L89.
Kahn, F. D. 1974, *Astr. Ap.*, **37**, 149.
Keene, J., Hildebrand, R. H., and Whitcomb, S. E. 1981, *IAU Symposium 96, Infrared Astronomy*, in preparation.
Kuiper, T. B. H., Rodriguez-Kuiper, E. N., and Zuckerman, B. 1978, *Ap. J.*, **219**, 129.
Kwan, J., and Scoville, N. 1976*a*, *Ap. J.*, **209**, 102.
_____. 1976*b*, *Ap. J.* (*Letters*), **210**, L39.
Larson, R. B. 1980, *M.N.R.A.S.*, **190**, 321.
Lüst, R., and Schlüter, A. 1955, *Zeitschrift für Astrophysik*, **38**, 190.
Martens, P. C. H. 1979, *Astr. Ap.*, **75**, L7.
Matsakis, D. N., Cheung, A. C., Wright, M. C. H., Askne, J. I. H., Townes, C. H., and Welch, W. J. 1980, *Ap. J.*, **236**, 481.
Menietti, J. D., and Fix, J. D. 1978, *Ap. J.*, **224**, 961.
Menon, T. K. 1961, *Pub. N.R.A.O.*, **1**, 1.
Morris, M., Palmer, P., and Zuckerman, B. 1980, *Ap. J.*, **237**, 1.
Morris, M., Redman, R., Reid, M. J., and Dickinson, D. F. 1979, *Ap. J.*, **229**, 257.
Nadeau, D., and Geballe, T. R. 1979, *Ap. J.* (*Letters*), **230**, L169.
Ney, E. P., and Merrill, K. W. 1977, *Bull. AAS*, **9**, 556.
Norris, R. P., Booth, R. S., and McLaughlin, W. 1980, in *Giant Molecular Clouds in the Galaxy*, ed. P. M. Solomon and M. G. Edmunds (Oxford: Pergamon Press), p. 193.
Phillips, J. P. 1979, *Astr. Ap.*, **71**, 115.
Phillips, T. G., Huggins, P. J., Neugebauer, G., and Werner, M. W. 1977, *Ap. J.* (*Letters*), **217**, L161.
Rieke, G. H., and Low, F. J. 1973, *Bull. AAS*, **4**, 436.
Rieke, G. H., Low, F. J., and Kleinmann, D. E. 1973, *Ap. J.* (*Letters*), **186**, L7.
Rodriguez, L. F., Ho, P. T. P., and Moran, J. M. 1980, *Bull. AAS*, **11**, 714.
Rydbeck, O. E. H., Hjalmarson, Å., Rydbeck, G., Ellder, J., Sume, A., and Lidholm, S. 1980, *IAU Symposium 87, Interstellar Molecules*, ed. B. Andrew (Dordrecht: Reidel), in press.
Schwartz, R. D. 1975, *Ap. J.*, **196**, 745.
Scoville, N. Z. 1980, *IAU Symposium 87, Interstellar Molecules*, ed. B. Andrew (Dordrecht: Reidel), in press.
Scoville, N. Z. 1981, *IAU Symposium 96, Infrared Astronomy*, ed. C. G. Wynn-Williams and D. Cruickshank (Dordrecht: Reidel), in press.
Scoville, N. Z., Hall, D. N. B., Kleinmann, S. G., and Ridgway, S. T. 1979, *Ap. J.* (*Letters*), **232**, L121.
Smithsonian Astrophysical Observatory Star Catalogue 1966, Part 3, (Washington D. C.: Smithsonian Institute) (SAO Catalogue).
Snell, R. L., Loren, R. B., and Plambeck, R. L. 1980, *Ap. J.* (*Letters*), **239**, L17.
Snyder, L. E., Dickinson, D. F., Brown, L. W., and Buhl, D. 1978, *Ap. J.*, **224**, 512.
Wannier, P. G., Philips, T. G., Higgins, P. J., and Knapp, G. R. 1980, *Bull. AAS*, **11**, 705.
Werner, M. W. Becklin, E. E., Gatley, I., and Neugebauer, G. 1977, in *Infrared and Submillimeter Astronomy*, ed. G. G. Fazio (Dordrecht: Reidel), p. 89.
Werner, M. W., Gatley, I., Harper, D. A., Becklin, E. E., Loewenstein, R. F., Telesco, C. M., and Thronson, H. A. 1976, *Ap. J.*, **204**, 420.
Westbrook, W. E., Werner, M. W., Elias, J. H., Gezari, D. Y., Hauser, M. G., Lo, K. Y., and Neugebauer, G. 1976, *Ap. J.*, **209**, 94.
Wilson, T. L., Downes, D., and Bieging, J. 1979, *Astr. Ap.*, **71**, 275.
Wright, A. E., and Barlow, M. J. 1975, *M.N.R.A.S.*, **170**, 41.
Wright, M. C. H., Welch, W. J., Vogel, S. N., Plambeck, R. L., Bieging, J. H., and Baud, B. 1980, *Bull. AAS*, **11**, 623.
Wynn-Williams, C. G. 1971, *M.N.R.A.S.*, **151**, 397.
Wynn-Williams, C. G., and Becklin, E. E. 1974, *Pub. A.S.P.*, **86**, 5.
Yorke, H. W., and Krügel, E. 1977, *Astr. Ap.*, **54**, 183.
Zappala, R. R., Becklin, E. E., Matthews, K., and Neugebauer, G. 1974, *Ap. J.*, **192**, 109.
Zuckerman, B., Kuiper, T. B. H., and Rodriguez-Kuiper, E. N. 1976, *Ap. J.* (*Letters*), **209**, L137.
Zuckerman, B., Palmer, P., and Morris, M. 1980, *Bull. AAS*, **12**, 483.

D. Downes: Institut de Radio Astronomie Millimetrique, 53 Avenue des Martyrs, B.P. 391, 38017 Grenoble Cedex, France

R. Genzel: Department of Physics, 563 Birge Hall, University of California, Berkeley, CA 94720

E. E. Becklin and C. G. Wynn-Williams: Institute for Astronomy, University of Hawaii, 2680 Woodlawn Drive, Honolulu, HI 96822

© American Astronomical Society • Provided by the NASA Astrophysics Data System